



Published in final edited form as:

Genes Brain Behav. 2017 November ; 16(8): 756–767. doi:10.1111/gbb.12391.

Phosphodiesterase-1b deletion confers depression-like behavioral resistance separate from stress-related effects in mice

Jillian R. Hufgard, Michael T. Williams, and Charles V. Vorhees*

Division of Neurology, Dept. of Pediatrics, Cincinnati Children's Research Foundation and University of Cincinnati College of Medicine, Cincinnati, OH, USA

Abstract

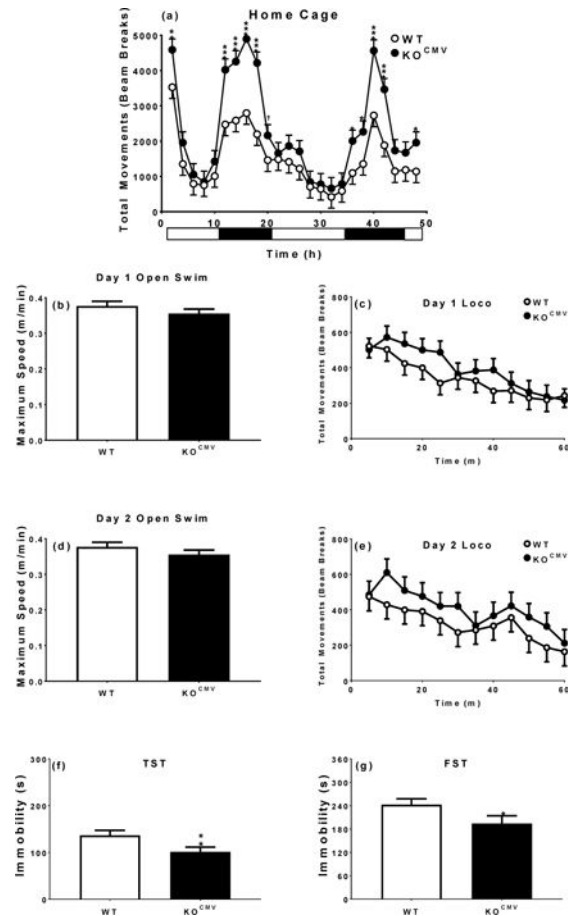
Phosphodiesterase-1b (Pde1b) is highly expressed in striatum, dentate gyrus, CA3, and substantia nigra. In a new Floxed *Pde1b* × Cre^{CMV} global knock-out (KO) mouse model we show an immobility resistance phenotype that recapitulates that found in constitutive *Pde1b* KO mice. We use this new mouse model to show that the resistance to acute stress-induced depression-like phenotype is not the product of changes in locomotor activity or reactivity to other stressors (learned helplessness, novelty suppressed feeding, or dexamethasone suppression), and is not associated with anhedonia using the sucrose preference test. Using tamoxifen inducible Cre, we show that the immobility-resistant phenotype depends on the age of induction. The effect is present when *Pde1b* is deleted from conception, P0 or P32, but not if deleted as adults (P60). We also mapped regional brain expression of PDE1B protein and of the Cre driver. These data add to the suggestion that PDE1B may be a target for drug development with therapeutic potential in depression alone or in combination with existing antidepressants.

Graphical abstract

We created a new Floxed *Pde1b* × Cre^{CMV} global knock-out (KO) mouse model and we show it to be immobility resistant in Forced Swim and Tail Suspension tests. We use this new mouse to show that the phenotype is not stress-related using tests of learned helplessness, novelty suppressed feeding, or dexamethasone suppression) nor anhedonic using the sucrose preference test. Using tamoxifen inducible Cre, we show that the immobility-resistant phenotype depends on age. The effect is present when *Pde1b* is deleted from conception, P0 or P32, but not if deleted in adults (P60). We mapped brain expression of PDE1B protein and Cre driver. The data suggest that PDE1B may be a target for drug development with potential antidepressant effects.

*Corresponding author: Charles V. Vorhees, Ph.D., Div. of Neurology (MLC 7044), Cincinnati Children's Research Foundation, 3333 Burnet Ave., Cincinnati, OH 45229, USA: charles.vorhees@cchmc.org. Tel: 513-636-8622; Fax: 513-636-3912.

Conflict of Interest Statement: The authors declare no conflicts of interest.



Keywords

Phosphodiesterase-1b; tail suspension test; forced swim test; striatum; dentate gyrus; critical period

Introduction

Major depression is the third leading cause of disability (WHO, 2008) and is predicted to be first by 2030 (Mathers *et al.*, 2008). Antidepressants fail to work for many patients creating the need to find new targets. Most antidepressants are presynaptic reuptake inhibitors and extend the action of serotonin (5-HT), dopamine (DA), and/or norepinephrine (NE). An alternative method of extending neurotransmitter action is prolonging postsynaptic signaling. Postsynaptic receptors activate second messengers (cAMP and cGMP) that in turn activate downstream targets such as protein kinase A (PKA), protein kinase G (PKG), exchange protein activated by cAMP, and cyclic nucleotide gated channels (Conti & Beavo, 2007). The duration of signaling is determined by the rate of cyclic nucleotide hydrolysis and is controlled by phosphodiesterases (PDEs). There are 11 PDE families composed of 21 genes. Each has a specific tissue distribution and selectivity (Maurice *et al.*, 2014).

Inhibition of PDE2 reverses impaired cognition caused by corticosterone or chronic stress (Xu *et al.*, 2013, Xu *et al.*, 2015). PDE4 inhibition using drugs, RNAi, or gene deletion decreases immobility in tail suspension (TST) and forced swim tests (FST) (Duman *et al.*, 1999, Fujita *et al.*, 2012, Jindal *et al.*, 2013, Jindal *et al.*, 2012, O'Donnell & Zhang, 2004, Schaefer *et al.*, 2012, Wang *et al.*, 2013, Zhang *et al.*, 2002). Clinical trials show that PDE4 inhibitors are effective antidepressants but have unacceptable side-effects (Hansen & Zhang, 2015). PDE5 inhibition increases antidepressant efficacy (Katarzyna *et al.*, 2012, Socafa *et al.*, 2012a, Socafa *et al.*, 2012b), and PDE10A has been linked to schizophrenia positive symptoms (Dlaboga *et al.*, 2008, Hebb & Robertson, 2007, Natesan *et al.*, 2014, Xu *et al.*, 2011), and haloperidol or clozapine treatment increases *Pde10a* expression (Xu *et al.*, 2013). PDE10A inhibition decreases stimulant-induced locomotor activity, blocks apomorphine-induced climbing, inhibits conditioned avoidance, blocks NMDA antagonist-induced deficits in acoustic startle, improves sensorimotor gating, increases sociability and social odor recognition, reverses stereotypy, and improves novel object recognition (Grauer *et al.*, 2009, Höfgen *et al.*, 2010, Schmidt *et al.*, 2008, Siuciak *et al.*, 2006a, Siuciak *et al.*, 2006b). These data support the potential of PDEs to modulate CNS function.

Pde1b is abundantly expressed in striatum, an area with involvement in stress and anxiety (Hufgard *et al.*, 2017, Kelly *et al.*, 2014, Lakics *et al.*, 2010). We showed that constitutive *Pde1b* knock-out (KO) mice have reduced immobility in TST and FST (Hufgard *et al.*, 2017), suggesting its potential as a drug target. These KO mice also show additive effects to two widely used antidepressants: fluoxetine, a selective serotonin reuptake inhibitor, and bupropion, a norepinephrine-dopamine reuptake inhibitor (Hufgard *et al.*, 2017). Constitutive KO mice have limitations on the types of hypotheses that may be tested because the genes are disrupted from conception and compensatory changes during development cannot be ruled-out. Therefore, we created a floxed *Pde1b* mouse that we describe here for the first time. First, floxed mice were crossed to a ubiquitous Cre line to create a global *Pde1b* KO mouse and these mice were compared with the constitutive *Pde1b* KO mice (Hufgard *et al.*, 2017) to ensure that the new model had the same phenotype. Next, the global *Pde1b* KO mice were used to test the role of PDE1B in response to stress. We then used a tamoxifen inducible Cre to determine the age of onset of the *Pde1b* KO mice immobility-resistant phenotype.

Methods

Animals and Husbandry

Mice were bred in-house in a pathogen free vivarium using Modular Animal Caging System (Alternative Design, Siloam Spring, AR) with HEPA filtered air at 30 air changes/h. Food and reverse-osmosis water were available ad libitum; cages had corncob bedding and cotton nest material. Mice were maintained on a 14:10 h light:dark cycle (lights on at 600 h). Protocols were approved by the Institutional Animal Care and Use Committee. The vivarium is accredited by AAALAC International. At weaning mice were housed with littermates by sex with 2–4 mice per cage. Mice were tested at ~postnatal day (P) 60 with not more than one mouse per genotype per sex per litter used. Mice were tested by personnel blind to genotype in the Animal Behavioral Core.

Generation of *Pde1b* ubiquitous conditional KO mice

Floxed mice were created on a C57BL/6J (albino) background. Flanking loxP sites were inserted between exons 2 and 3 and 5 and 6 with a neo cassette with flanking flippase recognition sites (Fig. 1A). Homologous recombination created a targeted allele with inserted LoxP sites and the neo cassette. Flippase recombinase was used to remove the neo cassette. The ubiquitous expressed cytomegalovirus (CMV) Cre driver, B6.C-Tg(CMV-cre)1Cgn/J, was used to create global *Pde1b* KO mice (KO^{CMV}). *Pde1b*^{flx/flx} × *Cre*^{+/-} mice were bred to create *Pde1b*^{-/-} × *Cre*^{+/-} offspring. These were bred with wildtype (WT) C57BL/6J mice to remove Cre. Thereafter, *Pde1b*^{+/-} × *Pde1b*^{+/-} breeding was used to generate WT, heterozygous (HET), and KO^{CMV} mice containing litters.

Western Blot Analysis

Western blots were used to confirm KO on brain samples of WT and KO^{CMV} mice; actin was used as reference (Fig. 1B). Frozen tissue was homogenized in radioimmuno-precipitation assay buffer (25 mM Tris, 150 mM NaCl, 0.5% sodium deoxychlorate, and 1% Triton X-100 adjusted to 7.2 pH with protease inhibitor (Pierce Biotechnology, Rockford, IL). Protein was quantified using the BCATM Protein Assay Kit (Pierce Biotechnology, Rockford, IL) and diluted to 3 µg/µL. Western blots were performed using LI-COR Odyssey® (LI-COR Biosciences, Lincoln, NE) procedures. Briefly, 25 µL of sample mixed with Laemmli buffer (Sigma, USA) were loaded in a 12% gel (Bio-Rad Laboratories, Hercules, CA) and run at 200 volts for 35 min in running buffer (25 mM Tris, 192 mM glycine, 0.1% SDS). The gel was then transferred to Immobilon-FL transfer membrane (Millipore, USA) in 1× rapid transfer buffer (AMRESCO, Solon, OH) at 40 V for 1.5 h. Membrane was soaked in Odyssey PBS blocking buffer for 1 h, primary antibody in blocking buffer with 0.2% Tween 20 incubated overnight at 4°C, secondary antibody incubated in blocking buffer with, 0.2% Tween 20, and 0.01% SDS for 1 h at room temperature. Antibodies were rabbit anti-PDE1B C-terminal (Ab170441 or Ab182565) at 1:500 or 1:5000, respectively, and mouse anti-actin (Ab3280) at 1:2000 as a loading control. Odyssey IRDye 680 and 800 secondary antibodies were used at a 1:15,000 dilution. Relative protein levels were quantified using the LI-COR Odyssey® scanner and Image Studio software that read the fluorescent intensity of the sample normalized to actin.

Fluorescent Immunohistochemistry

WT and KO^{CMV} mouse brains were perfused with 4% ice cold paraformaldehyde and stored overnight. Following at least 24 h in 30% sucrose they were cut on a freezing microtome at 20 µm and stained with cresyl violet. Free floating slices of prefrontal cortex, striatum, hippocampus, and substantia nigra were stained for PDE1B. Briefly, slices were washed in 1× PBS three times for 10 min a piece followed by blocking at 4°C in 2.5% donkey serum, 0.3% Triton X-100, 1% BSA in 1× PBS for 1 h. Primary antibodies were incubated in the blocking buffer overnight at 4°C and secondary was incubated for 1 h at room temperature in the dark. Rabbit anti-PDE1B (Ab182565) and Alexa Fluor 488 were used as primary (1:200) and secondary (1:500) antibodies with DAPI counterstain. Images were taken using a Nikon confocal microscope (Microscopy Imaging Core); all images are 4× magnification.

Open-Field

We used 40 × 40 cm activity chambers (PAS System, San Diego Instruments, San Diego, CA) (Hautman *et al.*, 2014). Mice were tested for 1 h and data recorded in 5 min intervals.

Tail Suspension Test

The method of Cryan *et al.* was used (Cryan *et al.*, 2005a). The mouse's tail was inserted through a hole in a transparent horizontal acrylic plate mounted on four legs and pulled snugly against the underneath surface so there was no space between the base of the tail and the plate. The test was scored in 1 min intervals for 5 min. Immobility (no movement) and latency to the first immobile episode were scored.

Forced Swim Test

Mice were placed in a glass cylindrical vessel 10 cm in diameter (i.d.), 25 cm tall filled to a depth of 6 cm with 22 ± 1 °C water and tested using a 2-day method (Cryan *et al.*, 2005b, Porsolt *et al.*, 1979). On day-1, mice were tested for 15 min and minutes 1–6 scored. On day-2, mice were tested for 5 min. Mice were scored for immobility, latency, and active swimming. Immobility was minimal movement sufficient to keep afloat.

Home Cage Activity

Mice were tested in standard cages, singly housed (Tang *et al.*, 2002). The home-cage system has metal frames with infrared photodetectors that surround the cage. Data were collected for 48 h (PAS System, San Diego Instruments, San Diego, CA).

Open Swim

We showed that constitutive *Pde1b* KO mice are more active than WT mice (Hufgard *et al.*, 2017), therefore, swimming activity was tested to determine if open-field activity generalized to swimming activity since the FST relies on swimming. Mice were placed in a 122 cm pool of water for 5 min and tracked using ANY-maze software (Stoelting, Wood Dale, IL) on two consecutive days.

Sucrose Preference

A sucrose preference test was used to assess anhedonia (Pothion *et al.*, 2004). Mice were adapted to drinking from a sipper sack for 7 days. Next, sacks were filled with 2% sucrose for 2 days, then they were returned to water for 5 more days. Mice were then given two sipper sacks, one with water and one with 2% sucrose, balanced for position across mice. Sacks were weighed before and 24 h later. Preference was: (sucrose solution ÷ sucrose + water) × 100.

Hot Plate

A 1 L beaker was placed on a hotplate at 100 °C. Mice were placed in the beaker and latency to paw licking or jumping was recorded (Eddy & Leimbach, 1953) up to a limit of 30 s.

Learned Helplessness

For learned helplessness (LH), mice of both genotypes were randomly assigned to shock or no-shock conditions (Mallesman *et al.*, 2012, Ridder *et al.*, 2005). Using a Gemini shuttle-box (SDI, San Diego, CA) helplessness was induced over two days by placing mice on one side and exposing them to 360 trials that consisted of a 0.3 mA scrambled shock through the grid floor that lasted 2 s with intertrial intervals (ITI) of variable lengths (1–10 s; averaging 5 s). Controls were placed in the apparatus for the same length of time but without shock. On day 3, mice were given 30 trials with 10 s ITIs. Trials consisted of the door opening and activation of foot shock for 24 s or until the mouse crossed into the non-shock side. Number of escapes and latency to escape were recorded.

Novelty Suppressed Feeding

Following LH, mice were food and water deprived for 24 h and presented with food for 10 min in a novel environment (Bessa *et al.*, 2009) that consisted of a 40 cm × 40 cm acrylic box. Latency to pellet investigation and amount eaten after returning to their home cage for 5 min were recorded.

Dexamethasone Suppression Test

Three days later, mice had blood collected by submandibular sampling. The next day they received a 3 µg/100 g body weight intraperitoneal injection of dexamethasone. Six hours later they were decapitated and blood collected (Ridder *et al.*, 2005). Blood was collected at the same time of day both times.

Corticosterone Analysis

Blood was collected in tubes containing 2% EDTA. Samples were kept on ice until spun at 610 RCF for 15 min at 4 °C. Plasma was removed and stored at –80 °C. Samples were assayed using one lot of Immunodiagnostic Systems ® Corticosterone EIA Kit in duplicate following the kit instructions.

Tamoxifen-induced PDE1B KO

Forebrain dominant calcium/calmodulin-dependent protein kinase II alpha (CaMKII α), a known regulator of PDE1B, Cre driver, B6.Cg- Tg(Camk2a-cre/ERT2)1Aibs/J, was used to create a tamoxifen inducible *Pde1b* mouse (Madisen *et al.*, 2010, Tsien *et al.*, 1996). *Pde1b*^{flox/flox} × Cre^{+/+} mice were bred to create *Pde1b*^{flox/flox} × Cre^{+/+} offspring. Recombination was initiated via tamoxifen administration. A subset of mice were also bred to a Gt(ROSA)26Sor^{tm14(CAG-tdTomato)Hze} mouse line to confirm expression of CaMKII α -cre using td-tomato fluorescence (red) and immunohistochemistry (IHC) staining of PDE1B (green). Western blots were used to verify PDE1B deletion.

Tamoxifen Administration

Male mice were gavaged with 20 mg/kg tamoxifen in 10 mL/kg of corn oil or corn oil alone for 5 days (Madisen *et al.*, 2010) beginning on P0, P32, or P60 (KO^(P0, P32, or P60)). No more than one male per group per age was used per litter. Mice were tested in open-field, TST, and FST as adults.

Experiments

Experiment-1—Experiment-1 was to test the global KO mice for consistency with the constitutive KO mice and determine the effects in HET mice. Accordingly, we used male WT, HET, and KO^{CMV} mice for open-field on day 1, TST on day 2, and FST on day 3 and 4 (N: WT=11, HET=8, KO^{CMV}=11 (Fig. 3a–c)). No differences were seen between WT and HET mice, therefore, HET mice were not tested further.

Experiment-2—Experiment-2 was to determine if the phenotype was also present in female mice. Accordingly, we compared female WT (n=14) and *Pde1b* KO^{CMV} (n=14) mice as in Experiment-1 (Fig. 3d–f). The immobility phenotype was similar in males and females, therefore, males were used in Experiment-3.

Experiment-3—Experiment-3 was designed to determine if the open-field increased activity in KO mice affected swimming activity. Accordingly, we tested both genotypes as follows: home-cage on day 1 and 2, open-swim on the morning of day 3 and open-field on the afternoon, repeat open-swim on the morning of day 4 and open-field on the afternoon, TST on day 5, and FST on day 6 and 7 (Fig. 4) (N: WT=11 and KO^{CMV}=12).

Experiment-4—Experiment-4 was designed to determine if the KO mice phenotype in TST and FST was associated with stress responsiveness or anhedonia. Accordingly, WT and *Pde1b* KO^{CMV} male mice were divided into subgroups for LH: WT/No Shock (n=10), WT/ Shock (n=14), KO^{CMV}/No Shock (n=11), KO^{CMV}/Shock (n=12). The sequence was: corticosterone assessment on day 1, sipper sack habituation on days 1–5, hot plate on day 6, sucrose preference on day 6–7, LH on days 7–9, repeat corticosterone assessment on day 8, 24 h food/water deprivation on day 9–10, novelty suppressed feeding on day 10, repeat sucrose preference on days 10–11, and dexamethasone suppression test on day 14 (Fig. 5).

Experiment-5—Experiment-5 was designed to determine the developmental onset of the immobility-resistant phenotype in KO mice. Accordingly, the experiment consisted of KO^{P0, P32, P60} mice (Fig. 6) tested as adults in open-field on day 1, TST on day 2, and FST on days 3–4 (Fig. 7). Group sizes were: WT^{P0} (n=14), KO^{P0} (n=16), WT^{P32} (n=12), KO^{P32} (n=12), WT^{P60} (n=10), and KO^{P60} (n=13).

Data Analysis

Data were analyzed using SAS (v9.3, SAS Institute, Cary, NC) with $p < 0.05$ as the threshold for significance. To control for litter, only one mouse per genotype per sex per litter was used. T-tests were used when there were two groups. When there were three groups, mixed linear ANOVA was used and data presented as least square mean (LS Means) \pm SEMs. Repeated measure Mixed model ANOVAs were used for corticosterone, home-cage, open-swim, and open-field and used the autoregressive-1 covariance structure and Kenward-Roger first order degrees of freedom. Litter was a random factor in these models.

Results

Generation of Global Knockout Mice

Whole brain western blots and IHC confirmed the deletion of PDE1B in the brain of *Pde1b* KO^{CMV} mice (Fig. 1b, Fig. 2a'–d'). We previously showed that *Pde1b* mRNA is highly expressed in the striatum (Hufgard *et al.*, 2017). In WT mice using IHC, we show little to no staining in the prefrontal cortex (Fig. 2a), confirmed the presence of PDE1B protein in striatum (Fig. 2b), show protein in the hippocampus in the dentate gyrus and CA3 (Fig 2c,d), and also in the substantia nigra (Fig. 2d).

Pde1b KO^{CMV} mice are healthy, well groomed, and not visibly different from WT mice.

Experiment 1: The male *Pde1b* KO^{CMV} mice do not differ from HET or WT littermates in open-field activity [$F(2,32.6)=0.8$, $p>0.4$] (Fig. 3a,c). Experiment 2: KO^{CMV} females were more active than WT littermates [$F(1,44.7)=6.1$, $p<0.05$] (Fig. 3b,d).

Acute Stress

Experiment 1—*Pde1b* KO^{CMV} mice showed decreased immobility in both TST [$F(2,28)=12.7$, $p<0.001$] (Fig. 3e) and FST [$F(2,27)=29.3$, $p<0.001$] (Fig. 3g) compared with WT and HET mice, thereby verifying that the *Pde1b* KO^{CMV} mice have the same phenotype as the constitutive KO mice (Hufgard *et al.*, 2017). Heterozygous male mice did not differ from WT mice; for this reason HET females were not tested.

Experiment 2—Female KO^{CMV} mice showed the same immobility as *Pde1b* KO^{CMV} males, i.e., they showed reduced immobility in the TST [$t(25)=3.0$, $p<0.01$] (Fig. 3f); however, in FST [$t(24)=0.8$, $p>0.05$] the effect was only a trend and not significant (Fig. 3h) compared with female WT mice.

Activity

Experiment 3—Since *Pde1b* KO mice are more active, we tested whether this had a diurnal component and whether open-field differences translate to swimming. For the former, home-cage activity was assessed and for the latter swimming activity. *Pde1b* KO^{CMV} mice showed greater increases in activity during the dark cycle compared with WT mice during the light cycle [Genotype \times Interval: $F(23,444)=2.2$, $p<0.01$] (Fig. 4a). However, when *Pde1b* KO^{CMV} mice were placed in an open pool of water, they showed no difference in swim speed (Fig. 4b and d) or distance traveled. A trend towards increased open-field activity was seen in *Pde1b* KO^{CMV} mice when compared with WT mice when tested for 1 h during the light cycle but the effect was not significant [Genotype \times Interval: $F(11,210)=1.6$, $p<0.10$] (Fig. 4c and e). Following these procedures, *Pde1b* KO^{CMV} mice still had decreased immobility in TST and FST compared with WT mice [TST: $t(19)=2.4$, $p<0.05$; FST day 1: $t(18)=1.9$, $p<0.05$] (Fig. 4f and g).

Sucrose Preference

Experiment 4—*Pde1b* KO^{CMV} and WT mice did not differ in the amount of water consumed when given water, but *Pde1b* KO^{CMV} mice (13.9 ± 1.4 g, consumed in 7 days) consumed more sucrose when given alone than WT mice (10.6 ± 0.6 g, consumed in 2 days)

[$t(21)=2.3$, $p<0.05$]. When a choice was presented, *Pde1b* KO^{CMV} mice did not differ in sucrose preference compared with WT mice (WT: $72.3 \pm 7.1\%$, KO: $64.2 \pm 7.8\%$).

Learned Helplessness

Before LH testing, mice were tested for pain thresholds on a hot plate. There were no differences in reactivity between groups (Fig. 5a). During the LH test, mice in the inescapable shock condition had longer escape latencies when escape was provided compared with no-shock groups [$F(1,105)=317.0$, $p<0.001$] (Fig. 5b). There were no differences in latency between WT and *Pde1b* KO^{CMV} mice on this test.

Novelty Suppressed Feeding and Sucrose Preference

For novelty suppressed feeding, latency to eat food (Fig. 5c) and the amount of food consumed (not shown) were not different across LH conditions or genotypes. Mice were also given a second sucrose preference test after 24 h food and water deprivation. There were no differences between LH and no-shock mice of either genotype (Fig. 5d).

There was an increase in corticosterone after the second day of LH between the no-shock and shock conditions, but there were no differences between the WT and KO^{CMV} groups (Fig. 5e). Corticosterone was not different among groups 5 days after LH (Fig. 5f, **left**). There were no differences in corticosterone 6 h after dexamethasone in KO^{CMV} vs. WT mice (Fig. 5f, **right**).

Critical Period

Experiment 5—*Pde1b* was selectively deleted in cells containing the CaMKII α promoter after tamoxifen exposure. Tamoxifen was started on P0, P32, or P60. There were no changes in general appearance or body weight from tamoxifen exposure. *Pde1b* KO mice at P32 and P60, but not at P0, showed reduced striatal PDE1B [P0: $t(3.0)=1.1$, $p>0.05$; P32: $t(2.0)=2.9$, $p<0.05$; P60: $t(1.3)=2.0$, $p<0.1$] (Fig. 6e, f, g, **left**). In the hippocampus PDE1B was reduced in KO mice at P0 and P32 but not at P60 [P0: $t(2.3)=3.5$, $p<0.05$; P32: $t(1.9)=3.0$, $p<0.05$; P60: $t(2.4)=1.3$, $p>0.05$] compared with WT mice (Fig. 6e, f, g, **right**). Figure 6a, b, c, d compares corn oil control and tamoxifen mice at P0 and shows reduction of PDE1B (green) and induction of ROSA (red) in striatum. *Pde1b* KO^{P0}, KO^{P32}, and KO^{P60} mice showed no differences from WT mice in open-field activity (not shown). *Pde1b* KO^{P0} mice had decreased immobility compared with WT littermates in FST [$t(27.7)=1.8$, $p<0.05$] (Fig. 7b), but not TST (Fig. 7a). *Pde1b* KO^{P32} mice had decreased immobility compared with WT in both TST and FST [TST: $t(21.9)=2.5$, $p<0.05$; FST: $t(21.4)=1.8$, $p<0.05$] (Fig. 7c, d). *Pde1b* KO^{P60} mice show no difference on either test (Fig. 7e, f).

Discussion

The antidepressant-like phenotype of constitutive *Pde1b* KO mice was described (Hufgard *et al.*, 2017). Constitutive *Pde1b* KO mice are resistant to the induction of immobility in both the TST and FST and show no PDE1A or PDE1C compensatory changes. We also showed that FST and chronic variable stress increases PDE1B protein expression in striatum and hippocampus in WT mice. Since constitutive models can cause compensatory changes or fail

to induce neuronal activity similarly to pharmacological targets, we developed a floxed mouse targeting *Pde1b* exons 3–5. *Pde1b* floxed mice were bred to CMV Cre mice to create a global *Pde1b* KO mouse. These mice recapitulated the phenotype of constitutive KO mice in both TST and FST, although the phenotype was more robust in males than females. By fluorescent IHC, PDE1B protein expression is highest in caudate-putamen, nucleus accumbens, dentate gyrus, CA3, and substantia nigra in WT mice. This is in agreement with prior protein and mRNA expression data in rats and humans and confirms that our global KO is specific to *Pde1b* (Kelly *et al.*, 2014, Lakics *et al.*, 2010, Polli & Kincaid, 1992, Polli & Kincaid, 1994, Yan *et al.*, 1994, Yu *et al.*, 1997).

In the global *Pde1b* KO line, spontaneous locomotor activity was increased but only in females during the diurnal phase as noted (Reed *et al.*, 2002). However, other data show increased activity before and after stimulant exposure in both sexes of global *Pde1b* KO mice (Ehrman *et al.*, 2006, Reed *et al.*, 2002, Siuciak *et al.*, 2007). Here, for the first time, we determined activity over a period of 48 h and found that *Pde1b* KO^{CMV} mice showed greater hyperactivity during the dark cycle. However, the nocturnal activity increase in *Pde1b* KO^{CMV} mice returned to WT mice levels during most of the light cycle.

To determine if increased spontaneous activity might contribute to the decreased TST and FST immobility in *Pde1b* KO mice, we tested activity in open-swim and open-field tests given the same day. *Pde1b* KO^{CMV} mice showed no differences in average or maximum swim speed, or distance traveled in an open pool of water. The same mice tested in TST and FST after open-swim and open-field still showed the immobility-resistant phenotype. This demonstrates that the *Pde1b* KO^{CMV} depression-resistant phenotype is not confounded by activity differences.

We questioned if the antidepressant-like phenotype of *Pde1b* KO^{CMV} mice was a byproduct of stress resistance since FST and TST both cause stress. We reasoned that if the underlying effect was stress-related then other stressors would also show a resistance phenotype. For this we used LH. Induction of LH caused longer escape latencies than in controls to escape the shock, but there were no differences in LH escape latencies between *Pde1b* KO^{CMV} and WT mice, indicating that the KO phenotype is not directly related to stress.

To further examine the depression-related phenotype of the *Pde1b* KO mice we used sucrose preference as a test of anhedonia. There were no differences between *Pde1b* KO^{CMV} and WT mice. As further tests, we used novelty suppressed feeding and dexamethasone suppression. Neither showed differences between *Pde1b* KO mice compared with WT mice, reinforcing the view that the KO phenotype is not stress-related.

When we deleted *Pde1b* at different ages, each of the early developmental deletions resulted in the antidepressant-like phenotype, i.e., when *Pde1b* was deleted by tamoxifen starting at P0 or P32, the same antidepressant-like phenotype was seen as in global *Pde1b* KO^{CMV} mice, but not in those that started tamoxifen at P60. If there are genetic variants of *PDE1B* in people (this is not yet known), this may suggest possible protective variations against depression as a function of inter-individual differences. Alternatively, early age phenotype induction could be the result of differences in Cre driver expression. Pyramidal cell

neurogenesis is embryonic and enters post-mitotic phases by P0 and are differentiated by P7 (Angevine Jr, 1965, Pokorný & Yamamoto, 1981a, Pokorný & Yamamoto, 1981b, Stanfield & Cowan, 1979). PDE1B is located in hippocampal pyramidal cells, therefore, P0 tamoxifen induction would take place during neurogenesis (Kincaid *et al.*, 1987). Further, expression of CaMKII α recombination at P29 is present in hippocampus, striatum, cortex, and Purkinje cells and differs from that prior to P29 (Tsien *et al.*, 1996). This change suggests that different populations of cells are more sensitive to recombination at different ages. Sometimes there are effects from tamoxifen inducible Cre, including leakage (non-tamoxifen induced expression) that may vary by age. Alternatively, age-dependent phenotype differences may reflect the lag between tamoxifen efficacy at deleting the gene and its effects on the emergence of the immobility phenotype that may not be the same at P0, P32, and P60. The antidepressant efficacy of current drugs in patients can take 4–6 weeks to reach full effect (Belzung, 2014). Whether this interacts with the age at which a protein's adult expression emerges, such as for PDE1B, is unknown.

In sum, PDE1B is expressed in areas associated with neuropsychiatric disorders, including depression (Lakics *et al.*, 2010). Our data further support the view that PDE1B may be a target for pharmacological intervention of depression.

Acknowledgments

This research was supported by NIH T32 ES007051.

References

- Angevine JB Jr. Time of neuron origin in the hippocampal region: An autoradiographic study in the mouse. *Experimental Neurology*. 1965
- Belzung C. Innovative Drugs to Treat Depression: Did Animal Models Fail to Be Predictive or Did Clinical Trials Fail to Detect Effects? *Neuropsychopharmacology*. 2014; 39:1041–1051. [PubMed: 24345817]
- Bessa J, Ferreira D, Melo I, Marques F, Cerqueira J, Palha J, Almeida O, Sousa N. The mood-improving actions of antidepressants do not depend on neurogenesis but are associated with neuronal remodeling. *Molecular psychiatry*. 2009; 14:764–773. [PubMed: 18982002]
- Conti M, Beavo J. Biochemistry and physiology of cyclic nucleotide phosphodiesterases: essential components in cyclic nucleotide signaling. *Annu Rev Biochem*. 2007; 76:481–511. [PubMed: 17376027]
- Cryan JF, Mombereau C, Vassout A. The tail suspension test as a model for assessing antidepressant activity: review of pharmacological and genetic studies in mice. *Neuroscience & Biobehavioral Reviews*. 2005a; 29:571–625. [PubMed: 15890404]
- Cryan JF, Valentino RJ, Lucki I. Assessing substrates underlying the behavioral effects of antidepressants using the modified rat forced swimming test. *Neuroscience & Biobehavioral Reviews*. 2005b; 29:547–569. [PubMed: 15893822]
- Dlaboga D, Hajjhussein H, O'Donnell JM. Chronic haloperidol and clozapine produce different patterns of effects on phosphodiesterase-1B, -4B, and -10A expression in rat striatum. *Neuropharmacology*. 2008; 54:745–754. [PubMed: 18222493]
- Duman RS, Malberg J, Thome J. Neural plasticity to stress and antidepressant treatment. *Biological psychiatry*. 1999; 46:1181–1191. [PubMed: 10560024]
- Eddy NB, Leimbach D. Synthetic analgesics. II. Dithienylbutenyl- and dithienylbutylamines. *Journal of Pharmacology and Experimental Therapeutics*. 1953; 107:385–393. [PubMed: 13035677]
- Ehrman L, Williams M, Schaefer T, Gudelsky G, Reed T, Fienberg A, Greengard P, Vorhees C. Phosphodiesterase 1B differentially modulates the effects of methamphetamine on locomotor

- activity and spatial learning through DARPP32-dependent pathways: evidence from PDE1B-DARPP32 double-knockout mice. *Genes, Brain and Behavior*. 2006; 5:540–551.
- Fujita M, Hines CS, Zoghbi SS, Mallinger AG, Dickstein LP, Liow JS, Zhang Y, Pike VW, Drevets WC, Innis RB. Downregulation of Brain Phosphodiesterase Type IV Measured with ¹¹C-(R)-Rolipram Positron Emission Tomography in Major Depressive Disorder. *Biological psychiatry*. 2012; 72:548–554. [PubMed: 22677471]
- Grauer SM, Pulito VL, Navarra RL, Kelly MP, Kelley C, Graf R, Langen B, Logue S, Brennan J, Jiang L. Phosphodiesterase 10A inhibitor activity in preclinical models of the positive, cognitive, and negative symptoms of schizophrenia. *Journal of Pharmacology and Experimental Therapeutics*. 2009; 331:574–590. [PubMed: 19661377]
- Hansen R, Zhang HT. Phosphodiesterase-4 modulation as a potential therapeutic for cognitive loss in pathological and non-pathological aging: possibilities and pitfalls. *Current pharmaceutical design*. 2015; 21:291–302. [PubMed: 25159075]
- Hautman ER, Kokenge AN, Udobi KC, Williams MT, Vorhees CV, Skelton MR. Female mice heterozygous for creatine transporter deficiency show moderate cognitive deficits. *Journal of inherited metabolic disease*. 2014; 37:63–68. [PubMed: 23716276]
- Hebb AL, Robertson HA. Role of phosphodiesterases in neurological and psychiatric disease. *Current opinion in pharmacology*. 2007; 7:86–92. [PubMed: 17113826]
- Höfgen N, Stange H, Schindler R, Lankau HJ, Grunwald C, Langen B, Egerland U, Tremmel P, Pangalos MN, Marquis KL. Discovery of imidazo [1, 5-a] pyrido [3, 2-e] pyrazines as a new class of phosphodiesterase 10A inhibitors. *Journal of medicinal chemistry*. 2010; 53:4399–4411. [PubMed: 20450197]
- Hufgard JR, Williams MT, Skelton MR, Grubisha O, Ferreira FM, Sanger H, Wright ME, Reed-Kessler TM, Rasmussen K, Duman RS, Vorhees CV. Phosphodiesterase-1b (Pde1b) knockout mice are resistant to forced swim and tail suspension induced immobility and show upregulation of Pde10a. *Psychopharmacology*. 2017
- Jindal A, Mahesh R, Bhatt S. Etazolate, a phosphodiesterase 4 inhibitor reverses chronic unpredictable mild stress-induced depression-like behavior and brain oxidative damage. *Pharmacology Biochemistry and Behavior*. 2013; 105:63–70.
- Jindal A, Mahesh R, Gautam B, Bhatt S, Pandey D. Antidepressant-like effect of etazolate, a cyclic nucleotide phosphodiesterase 4 inhibitor—an approach using rodent behavioral antidepressant tests battery. *European journal of pharmacology*. 2012; 689:125–131. [PubMed: 22698578]
- Katarzyna S, Dorota N, Ewa P, Piotr W. Influence of the phosphodiesterase type 5 inhibitor, sildenafil, on antidepressant-like activity of magnesium in the forced swim test in mice. *Pharmacological Reports*. 2012; 64:205–211. [PubMed: 22580537]
- Kelly MP, Adamowicz W, Bove S, Hartman AJ, Mariga A, Pathak G, Reinhart V, Romegialli A, Kleiman RJ. Select 3', 5'-cyclic nucleotide phosphodiesterases exhibit altered expression in the aged rodent brain. *Cellular signalling*. 2014; 26:383–397. [PubMed: 24184653]
- Kincaid RL, Balaban CD, Billingsley ML. Differential localization of calmodulin-dependent enzymes in rat brain: evidence for selective expression of cyclic nucleotide phosphodiesterase in specific neurons. *Proceedings of the National Academy of Sciences*. 1987; 84:1118–1122.
- Lakics V, Karran EH, Boess FG. Quantitative comparison of phosphodiesterase mRNA distribution in human brain and peripheral tissues. *Neuropharmacology*. 2010; 59:367–374. [PubMed: 20493887]
- Madisen L, Zwingman TA, Sunkin SM, Oh SW, Zariwala HA, Gu H, Ng LL, Palmiter RD, Hawrylycz MJ, Jones AR. A robust and high-throughput Cre reporting and characterization system for the whole mouse brain. *Nature neuroscience*. 2010; 13:133–140. [PubMed: 20023653]
- Malkesman O, Austin D, Tragon T, Henter I, Reed J, Pellicchia M, Chen G, Manji H. Targeting the BH3-interacting domain death agonist to develop mechanistically unique antidepressants. *Molecular psychiatry*. 2012; 17:770–780. [PubMed: 21727899]
- Mathers, C., Fat, DM., Boerma, JT. The global burden of disease: 2004 update. World Health Organization; 2008.
- Maurice DH, Ke H, Ahmad F, Wang Y, Chung J, Manganiello VC. Advances in targeting cyclic nucleotide phosphodiesterases. *Nature Reviews Drug Discovery*. 2014; 13:290–314. [PubMed: 24687066]

- Natesan S, Ashworth S, Nielsen J, Tang S, Salinas C, Kealey S, Lauridsen J, Stensbøl T, Gunn R, Rabiner E. Effect of chronic antipsychotic treatment on striatal phosphodiesterase 10A levels: a [11C] MP-10 PET rodent imaging study with ex vivo confirmation. *Translational psychiatry*. 2014; 4:e376. [PubMed: 24690597]
- O'Donnell JM, Zhang HT. Antidepressant effects of inhibitors of cAMP phosphodiesterase (PDE4). *Trends in Pharmacological Sciences*. 2004; 25:158–163. [PubMed: 15019272]
- Pokorný J, Yamamoto T. Postnatal ontogenesis of hippocampal CA1 area in rats. I. Development of dendritic arborisation in pyramidal neurons. *Brain research bulletin*. 1981a; 7:113–120. [PubMed: 7272792]
- Pokorný J, Yamamoto T. Postnatal ontogenesis of hippocampal CA1 area in rats. II. Development of ultrastructure in stratum lacunosum and moleculare. *Brain research bulletin*. 1981b; 7:121–130. [PubMed: 7272793]
- Polli JW, Kincaid RL. Molecular cloning of DNA encoding a calmodulin-dependent phosphodiesterase enriched in striatum. *Proceedings of the National Academy of Sciences*. 1992; 89:11079–11083.
- Polli JW, Kincaid RL. Expression of a calmodulin-dependent phosphodiesterase isoform (PDE1B1) correlates with brain regions having extensive dopaminergic innervation. *The Journal of neuroscience*. 1994; 14:1251–1261. [PubMed: 8120623]
- Porsolt RD, Bertin A, Blavet N, Deniel M, Jalfre M. Immobility induced by forced swimming in rats: effects of agents which modify central catecholamine and serotonin activity. *European journal of pharmacology*. 1979; 57:201–210. [PubMed: 488159]
- Pothion S, Bizot JC, Trovero F, Belzung C. Strain differences in sucrose preference and in the consequences of unpredictable chronic mild stress. *Behavioural brain research*. 2004; 155:135–146. [PubMed: 15325787]
- Reed TM, Repaske DR, Snyder GL, Greengard P, Vorhees CV. Phosphodiesterase 1B knock-out mice exhibit exaggerated locomotor hyperactivity and DARPP-32 phosphorylation in response to dopamine agonists and display impaired spatial learning. *The Journal of neuroscience*. 2002; 22:5188–5197. [PubMed: 12077213]
- Ridder S, Chourbaji S, Hellweg R, Urani A, Zacher C, Schmid W, Zink M, Hörtnagl H, Flor H, Henn FA. Mice with genetically altered glucocorticoid receptor expression show altered sensitivity for stress-induced depressive reactions. *The Journal of neuroscience*. 2005; 25:6243–6250. [PubMed: 15987954]
- Schaefer T, Braun A, Amos-Kroohs R, Williams M, Ostertag E, Vorhees C. A new model of Pde4d deficiency: genetic knock-down of PDE4D enzyme in rats produces an antidepressant phenotype without spatial cognitive effects. *Genes, Brain and Behavior*. 2012; 11:614–622.
- Schmidt CJ, Chapin DS, Cianfrogna J, Corman ML, Hajos M, Harms JF, Hoffman WE, Lebel LA, McCarthy SA, Nelson FR. Preclinical characterization of selective phosphodiesterase 10A inhibitors: a new therapeutic approach to the treatment of schizophrenia. *Journal of Pharmacology and Experimental Therapeutics*. 2008; 325:681–690. [PubMed: 18287214]
- Siuciak JA, Chapin DS, Harms JF, Lebel LA, McCarthy SA, Chambers L, Shrikhande A, Wong S, Menniti FS, Schmidt CJ. Inhibition of the striatum-enriched phosphodiesterase PDE10A: a novel approach to the treatment of psychosis. *Neuropharmacology*. 2006a; 51:386–396. [PubMed: 16780899]
- Siuciak JA, McCarthy SA, Chapin DS, Fujiwara RA, James LC, Williams RD, Stock JL, McNeish JD, Strick CA, Menniti FS. Genetic deletion of the striatum-enriched phosphodiesterase PDE10A: evidence for altered striatal function. *Neuropharmacology*. 2006b; 51:374–385. [PubMed: 16769090]
- Siuciak JA, McCarthy SA, Chapin DS, Reed T, Vorhees C, Repaske D. Behavioral and neurochemical characterization of mice deficient in the phosphodiesterase-1B (PDE1B) enzyme. *Neuropharmacology*. 2007; 53:113–124. [PubMed: 17559891]
- Socala K, Nieoczym D, Wyska E, Poleszak E, Wla P. Sildenafil, a phosphodiesterase type 5 inhibitor, enhances the activity of two atypical antidepressant drugs, mianserin and tianeptine, in the forced swim test in mice. *Progress in Neuro-Psychopharmacology and Biological Psychiatry*. 2012a; 38:121–126. [PubMed: 22406168]

- Socala K, Nieoczym D, Wyska E, Poleszak E, Wla P. Sildenafil, a phosphodiesterase type 5 inhibitor, enhances the antidepressant activity of amitriptyline but not desipramine, in the forced swim test in mice. *Journal of Neural Transmission*. 2012b; 119:645–652. [PubMed: 22215207]
- Stanfield BB, Cowan WM. The development of the hippocampus and dentate gyrus in normal and reeler mice. *Journal of Comparative Neurology*. 1979; 185:423–459. [PubMed: 86549]
- Tang X, Orchard SM, Sanford LD. Home cage activity and behavioral performance in inbred and hybrid mice. *Behavioural brain research*. 2002; 136:555–569. [PubMed: 12429418]
- Tsien JZ, Chen DF, Gerber D, Tom C, Mercer EH, Anderson DJ, Mayford M, Kandel ER, Tonegawa S. Subregion- and Cell Type-Restricted Gene Knockout in Mouse Brain. *Cell*. 1996; 87:1317–1326. [PubMed: 8980237]
- Wang ZZ, Zhang Y, Liu YQ, Zhao N, Zhang YZ, Yuan L, An L, Li J, Wang XY, Qin JJ. RNA interference-mediated phosphodiesterase 4D splice variants knock-down in the prefrontal cortex produces antidepressant-like and cognition-enhancing effects. *British journal of pharmacology*. 2013; 168:1001–1014. [PubMed: 23003922]
- Xu Y, Pan J, Chen L, Zhang C, Sun J, Li J, Nguyen L, Nair N, Zhang H, O'Donnell JM. Phosphodiesterase-2 inhibitor reverses corticosterone-induced neurotoxicity and related behavioural changes via cGMP/PKG dependent pathway. *International Journal of Neuropsychopharmacology*. 2013; 16:835–847. [PubMed: 22850435]
- Xu Y, Pan J, Sun J, Ding L, Ruan L, Reed M, Yu X, Lin D, Li J, Chen L. Inhibition of phosphodiesterase 2 reverses impaired cognition and neuronal remodeling caused by chronic stress. *Neurobiology of aging*. 2015; 36:955–970. [PubMed: 25442113]
- Xu, Y., Zhang, HT., O'Donnell, JM. Phosphodiesterases as Drug Targets. Springer; 2011. Phosphodiesterases in the central nervous system: implications in mood and cognitive disorders; p. 447-485.
- Yan C, Bentley JK, Sonnenburg WK, Beavo JA. Differential expression of the 61 kDa and 63 kDa calmodulin-dependent phosphodiesterases in the mouse brain. *The Journal of neuroscience*. 1994; 14:973–984. [PubMed: 8120637]
- Yu J, Wolda SL, Frazier AL, Florio VA, Martins TJ, Snyder PB, Harris EA, McCaw KN, Farrell CA, Steiner B. Identification and characterisation of a human calmodulin-stimulated phosphodiesterase PDE1B1. *Cellular signalling*. 1997; 9:519–529. [PubMed: 9419816]
- Zhang HT, Huang Y, Jin SC, Frith SA, Suvarna N, Conti M, James M. Antidepressant-like profile and reduced sensitivity to rolipram in mice deficient in the PDE4D phosphodiesterase enzyme. *Neuropsychopharmacology*. 2002; 27:587–595. [PubMed: 12377395]

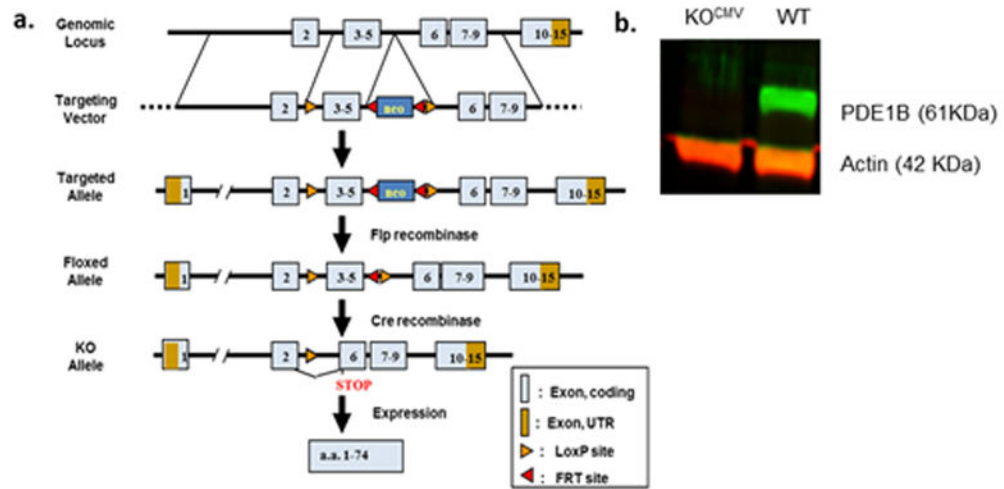


Figure 1. Generation of floxed mice and confirmation of global knockout mice (KO^{CMV}). **a.** Schematic of the Floxed mouse model. **b.** Whole brain western blot confirmation of complete lack of PDE1B in KO^{CMV} mice.

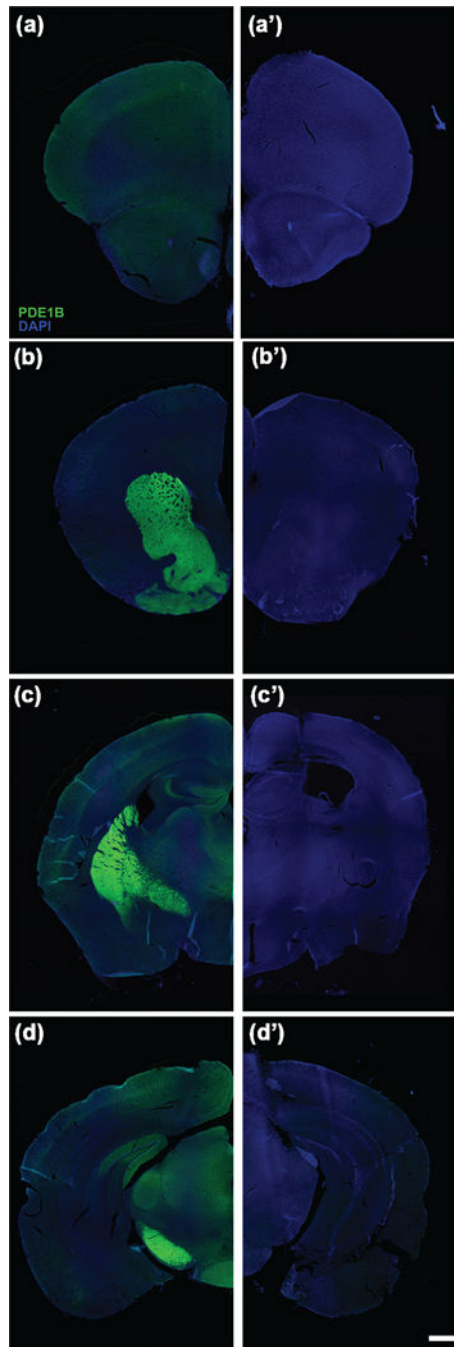


Figure 2. Fluorescent immunohistochemistry analysis of PDE1B in the brain localizes to regions related to stress and depression. **a.** WT prefrontal cortex. **a'.** KO^{CMV} prefrontal cortex. **b.** WT striatum. **b'.** KO^{CMV} striatum. **c.** WT hippocampus. **c'.** KO^{CMV} hippocampus. **d.** WT substantia nigra. **d'.** KO^{CMV} substantia nigra. DAPI=Blue and PDE1B=Green. Scale = 1000 μ m.

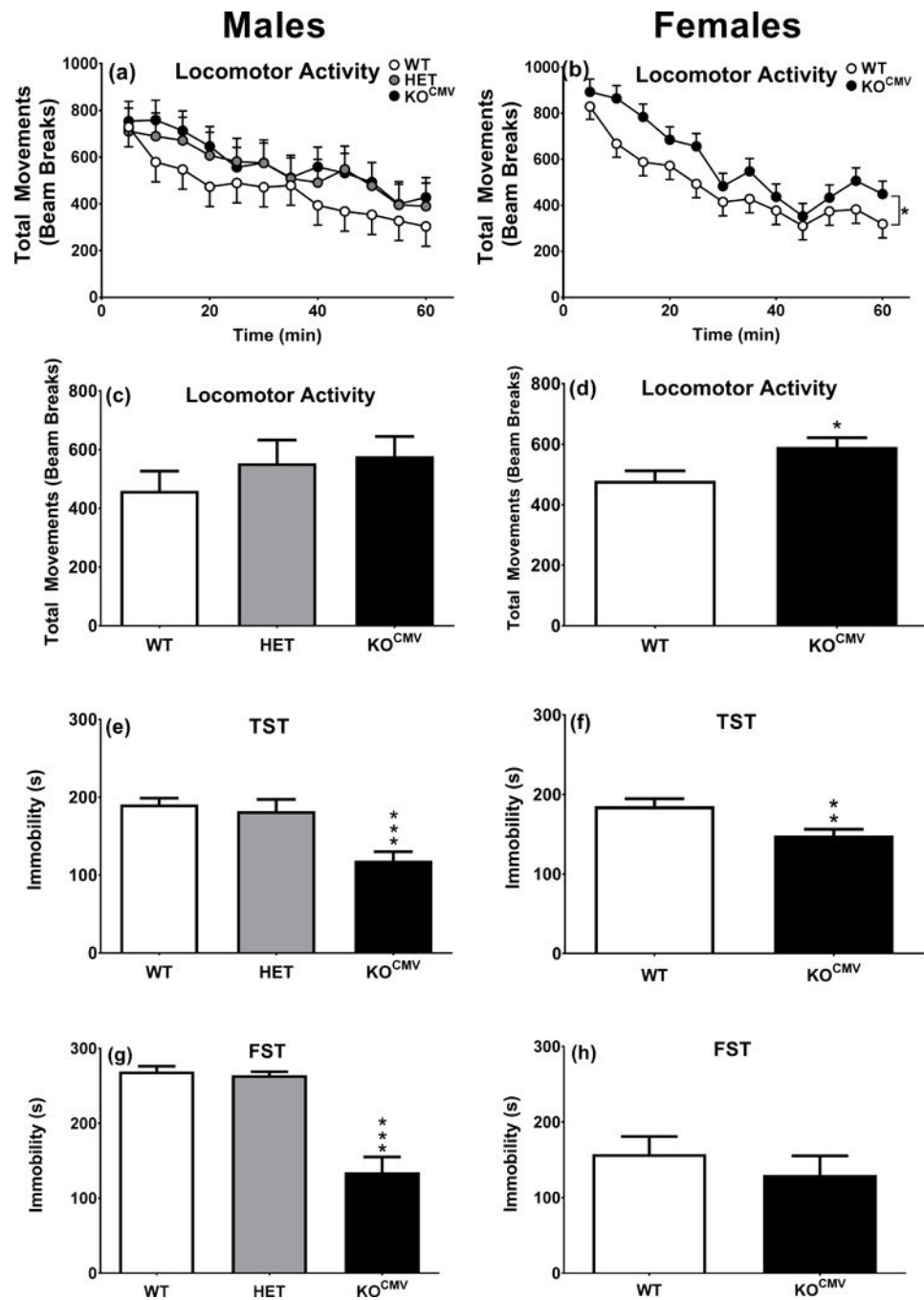


Figure 3. KO^{CMV} mice have decreased immobility time in depression-related tasks compared with control littermates. **a.** Locomotor activity males genotype*interval (WT n=11, HET n=8, KO^{CMV} n=11). **b.** Locomotor activity females genotype*interval (WT n=14, KO^{CMV} n=14). **c.** Locomotor activity males. **d.** Locomotor activity females. **e.** TST males (WT n=11, HET n=8, KO^{CMV} n=10). **f.** TST females (WT n=13, KO^{CMV} n=14). **g.** FST day 2, 5 min for males (WT n=9, HET n=8, KO^{CMV} n=11). **h.** FST day 2, 5 min for females (WT n=13, KO^{CMV} n=13). *p 0.05, **p 0.01, and ***p 0.001.

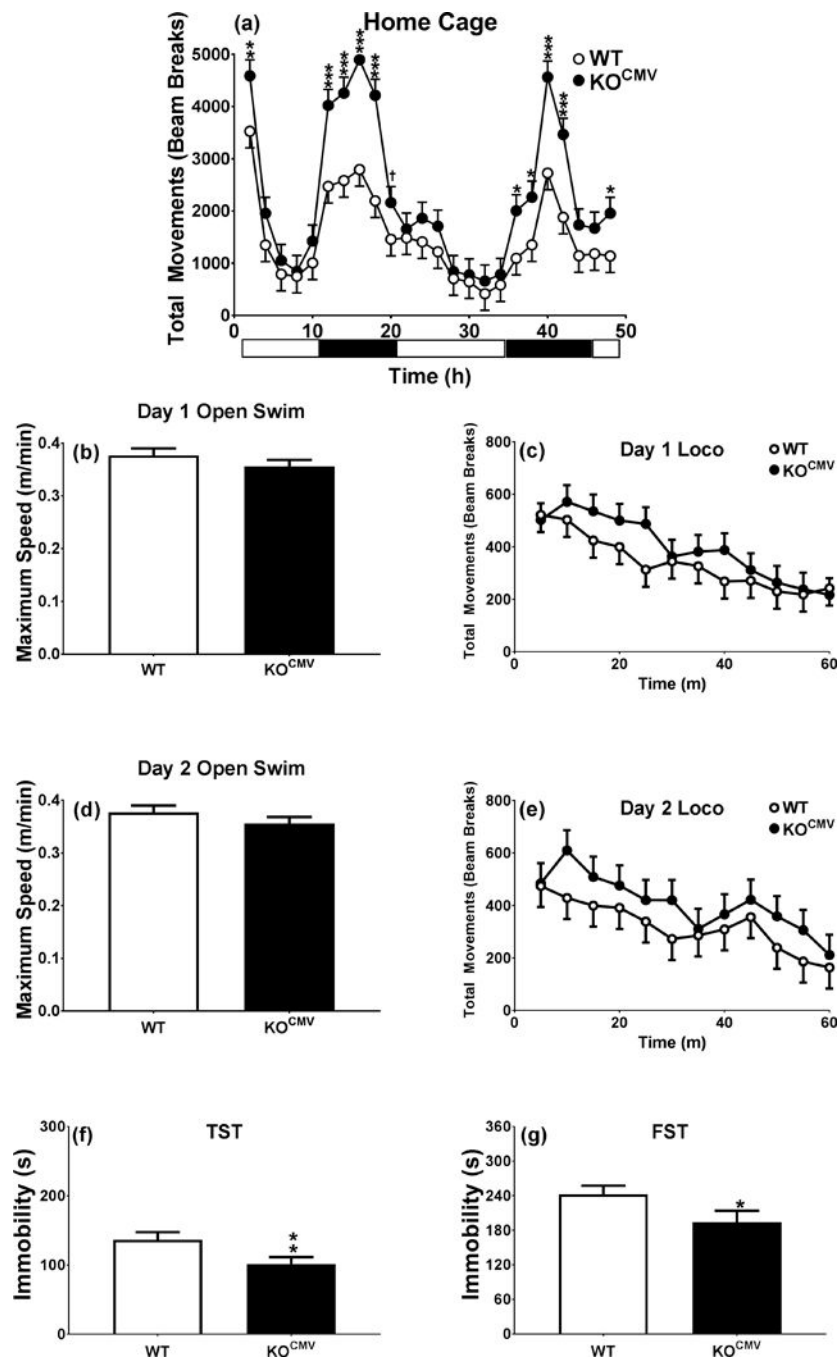


Figure 4. *Pde1b* KO^{CMV} mice are hyperactive at night and when introduced to the novel home cage, although land hyperactivity did not predict water hyperactivity. **a.** 48 h home cage (WT n=11, KO^{CMV} n=12). **b.** Day 1, 5 min open swim (WT n=11, KO^{CMV} n=12). **c.** 1 h locomotor activity day 1 (WT n=11, KO^{CMV} n=12). **d.** Day 2, 5 min open swim (WT n=11, KO^{CMV} n=12). **e.** 1 h locomotor activity day 2 (WT n=11, KO^{CMV} n=12). **f.** 5 min TST (WT n=10, KO^{CMV} n=11). **g.** 6 min FST (WT n=9, KO^{CMV} n=11). †p < 0.1, *p < 0.05, **p < 0.01, ***p < 0.001.

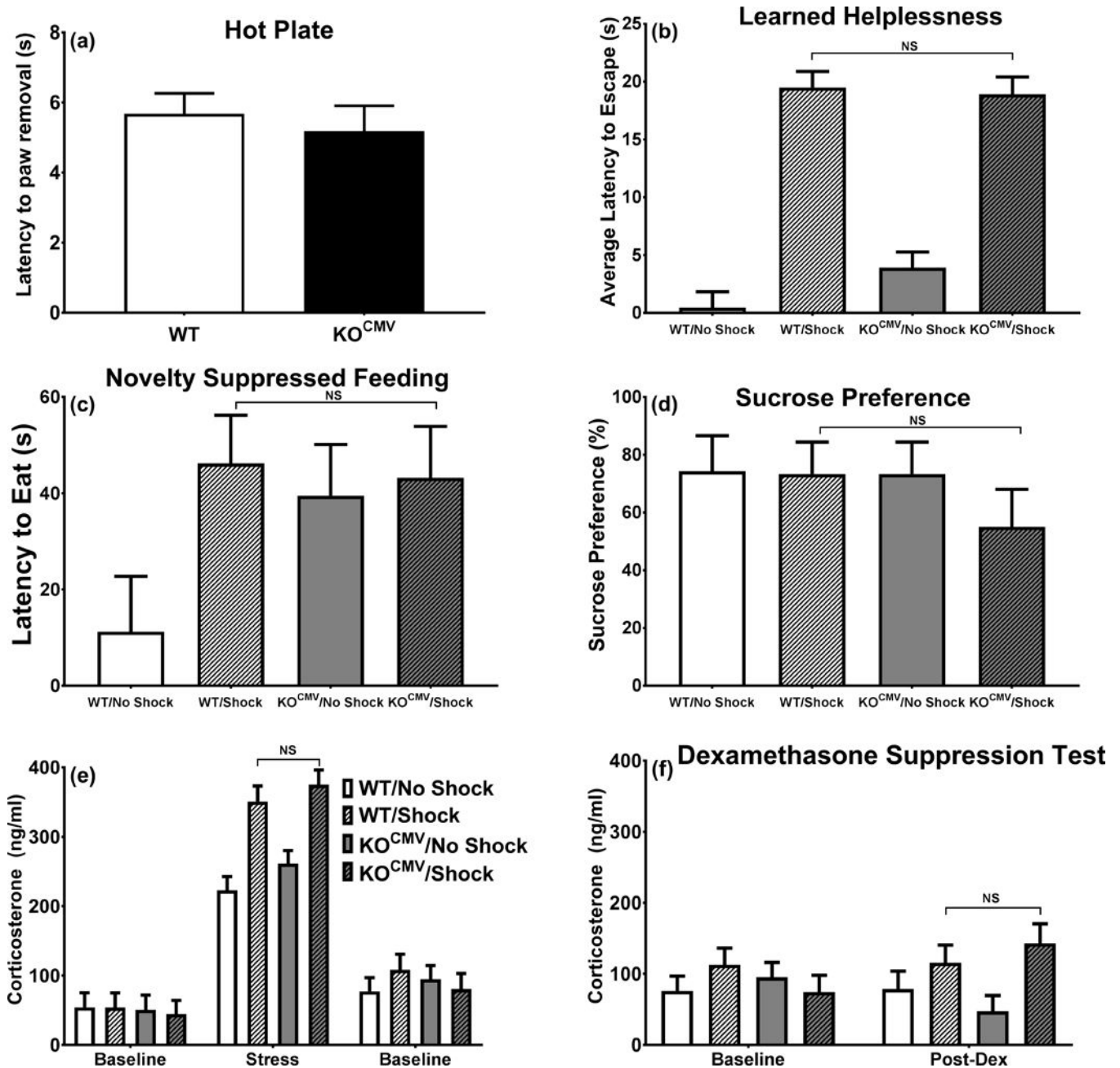


Figure 5. *Pde1b* KO^{CMV} mice do not differ from WT littermates when exposed to the learned helplessness procedure. **a.** Latency to remove paw from hot plate (WT $n=22$, KO^{CMV} $n=21$). **b.** Latency to escape shock (WT/No Shock $n=10$, WT/Shock $n=11$, KO^{CMV} /No Shock $n=10$, KO^{CMV} /Shock $n=8$). **c.** Latency to eat in a novel environment (WT/No Shock $n=8$, WT/Shock $n=12$, KO^{CMV} /No Shock $n=10$, KO^{CMV} /Shock $n=11$). **d.** Sucrose preference following 24 h food and water deprivation (WT/No Shock $n=10$, WT/Shock $n=14$, KO^{CMV} /No Shock $n=11$, KO^{CMV} /Shock $n=12$). **e.** Plasma corticosterone response before, during, and after LH exposure (WT/No Shock $n=9$, WT/Shock $n=9$, KO^{CMV} /No Shock $n=9$,

KO^{CMV}/Shock n=8). **f.** Plasma corticosterone following dexamethasone (WT/No Shock n=8, WT/Shock n=8, KO^{CMV}/No Shock n=8, KO^{CMV}/Shock n=7).

Author Manuscript

Author Manuscript

Author Manuscript

Author Manuscript

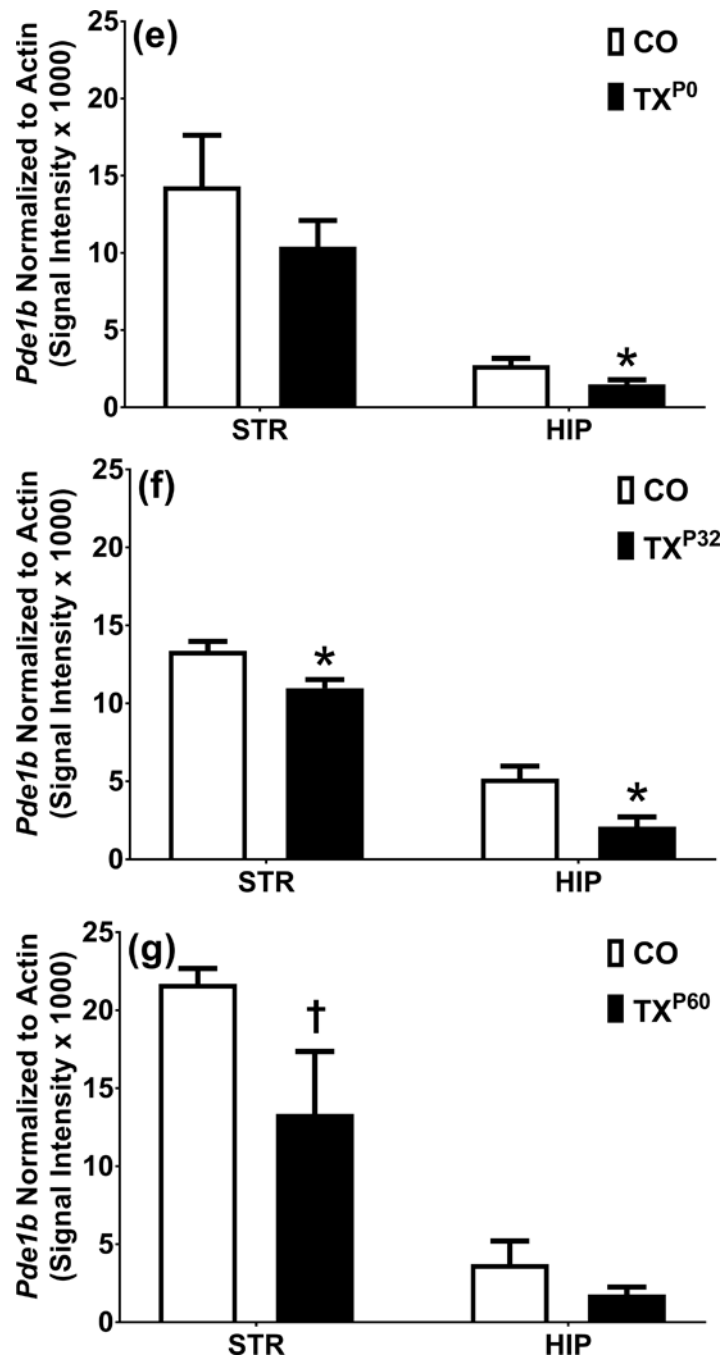


Figure 6. Analysis of localization and quantity of PDE1B in KO^{P0, P32, P60} mice. **a.** Expression pattern of CaMKII α Cre driver and PDE1B in striatum of P0 corn oil dosed mice. **a'.** Expression pattern of CaMKII α Cre driver and PDE1B in striatum of P0 tamoxifen dosed mice. **b.** DAPI corn oil. **b'.** DAPI tamoxifen. **c.** PDE1B corn oil. **c'.** PDE1B tamoxifen. **d.** ROSA corn oil. **d'.** ROSA tamoxifen. **e.** Western blot analysis of striatum and hippocampus in P0 dosed mice. **f.** Western blot analysis of striatum and hippocampus in P32 dosed mice. **g.**

Western blot analysis of striatum and hippocampus in P60 dosed mice. Blue = DAPI, Green = PDE1B, Red = Td-Tomato. 2000 μm . † $p < 0.1$ and * $p < 0.05$.

Author Manuscript

Author Manuscript

Author Manuscript

Author Manuscript

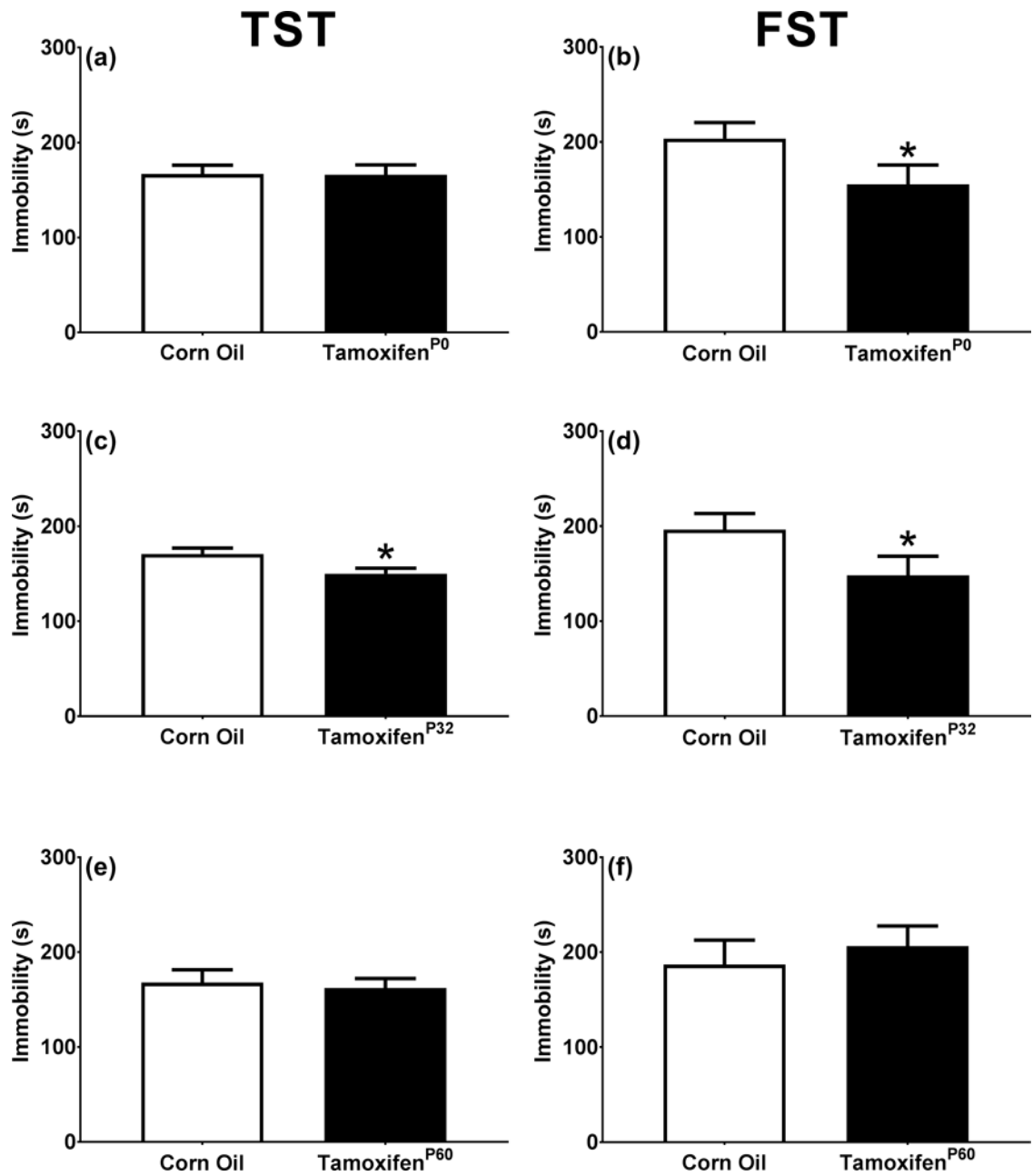


Figure 7.

When PDE1B is removed prior to sexual maturity KO mice had a reduction in immobility time in the TST and the FST. **a.** KO^{P0} Tail suspension test (WT n=14, KO^{P0} n=16). **b.** KO^{P0} Forced swim test (WT n=14, KO^{P0} n=16). **c.** KO^{P32} Tail suspension test (WT n=12, KO^{P32} n=12). **d.** KO^{P32} Forced swim test (WT n=12, KO^{P32} n=12). **e.** KO^{P60} Tail suspension test (WT n=10, KO^{P60} n=13). **f.** KO^{P60} Forced swim test (WT n=10, KO^{P60} n=13). *p < 0.05